Optimal design and fabrication method for antireflection coatings for *P*-polarized 193 nm laser beam at large angles of incidence (68°–74°)

Jingcheng Jin,[1,2] Chunshui Jin,[1,*] Chun Li,[1] Wenyuan Deng,[1] and Yanhe Chang[1,2]

[1]*State Key Laboratory of Applied Optics, Changchun Institute of Optics, Fine Mechanics and Physics, Chinese Academy of Sciences, Changchun, Jilin 130033, China*

[2]*Graduate University of Chinese Academy of Sciences, Beijing 100039, China*

**Corresponding author: jin_chunshui@aliyun.com*

Received June 10, 2013; revised July 11, 2013; accepted July 19, 2013;
posted July 19, 2013 (Doc. ID 191889); published August 8, 2013

Most of the optical axes in modern systems are bent for optomechanical considerations. Antireflection (AR) coatings for polarized light at oblique incidence are widely used in optical surfaces like prisms or multiform lenses to suppress undesirable reflections. The optimal design and fabrication method for AR coatings with large-angle range (68°–74°) for a *P*-polarized 193 nm laser beam is discussed in detail. Experimental results showed that after coating, the reflection loss of a *P*-polarized laser beam at large angles of incidence on the optical surfaces is reduced dramatically, which could greatly improve the output efficiency of the optical components in the deep ultraviolet vacuum range.

OCIS codes: (310.1210) Antireflection coatings; (310.5448) Polarization, other optical properties; (310.6805) Theory and design.

http://dx.doi.org/10.1364/JOSAA.30.001768

1. INTRODUCTION

ArF excimer lasers have been increasingly applied in semiconductor exposure, material microstructuring, and medical surgeries because of their high power, high homogeneity, and high stability [1]. Improvements to ArF excimer lasers, including higher output power (>90 W), frequency (>6 kHz), and enhancements on beam homogeneity and pulse stability, are continuing to be developed. Especially in the semiconductor industry, the 193 nm ArF lithography technology is extending for higher resolution below 22 nm node, which makes an ever-growing demand for the coating components inside the system. The coating components can stand long duration exposure to ultraviolet radiation without significant change in performance. For example, in the line narrowing module of an ArF excimer laser cavity, the hypotenuse surfaces of the expanding prisms are coated with antireflection (AR) coatings for *P*-polarized light to reduce the reflection loss [2–5]. In order to obtain enough expanding ratio, the incidence angle on the hypotenuse of the expanding prisms needs to be as big as possible. But the residual reflection loss on the bare surfaces could be sufficiently high. Low output efficiency or failure of the cavity could result from these reflection losses. Considering the increasing difficulty and cost of AR coating processes as the incidence angle gets bigger, the design incidence angles are usually selected larger than the Brewster's angle. The AR coatings for a *P*-polarized 193 nm laser beam in the large-angle range (68°–74°) were designed and fabricated here in detail, which could meet most of the needs and offering delightful angle tolerance of assembling optical path units. The case of an angle of incidence (AOI) equal to 74° used as an example in the following illustration and analysis, and the optical performance of this AR coating was tested and analyzed.

2. COATING DESIGN

The main challenge in fabricating AR coatings for a *P*-polarized laser beam at 193 nm for oblique incidence can be derived from the aspects as follows: the minimizing of heavy absorption problem, which is a key factor for the deep ultraviolet vacuum (DUV) coatings [6,7]; in the case of an extreme large AOI (larger than the Brewster's angle), the reflection reduction efficiency of the stack of quarter-wave layers is reduced dramatically so that the required number of layers is substantially increased and the optical constants and thickness tolerance on each layer are greatly tightened [8,9].

A. Optical Constants

The AR coatings were deposited using the thermal evaporation method in a Leybold DUV batch coater. Low-oxide lanthanum fluoride (LaF_3) and magnesium fluoride (MgF_2) were used as H and L materials (H, L stand for "quarter-wave" layer thickness). Excimer grade CaF_2 (111) (rms < 0.3 nm) was used as substrates. Thin film software Optilayer based on Needle optimization technology is used for the design and analysis of the coating system [10].

Single layers of H and L materials are deposited and analyzed to obtain the optical constants. The optical constants (refractive index and extinction coefficient) of LaF_3 are difficult to obtain because of its inhomogeneity. Reliable estimation of optical constants in LaF_3 layers is essential to the *P*-polarized AR coatings for large AOI, which requires high accuracy of the thickness and density of an individual layer. A first-order bulk inhomogeneity (Schroeder model) was assumed to calculate the optical constants of LaF_3. This model implies that the film refractive index changes linearly from the film substrate side to the film ambient side. It can be discerned

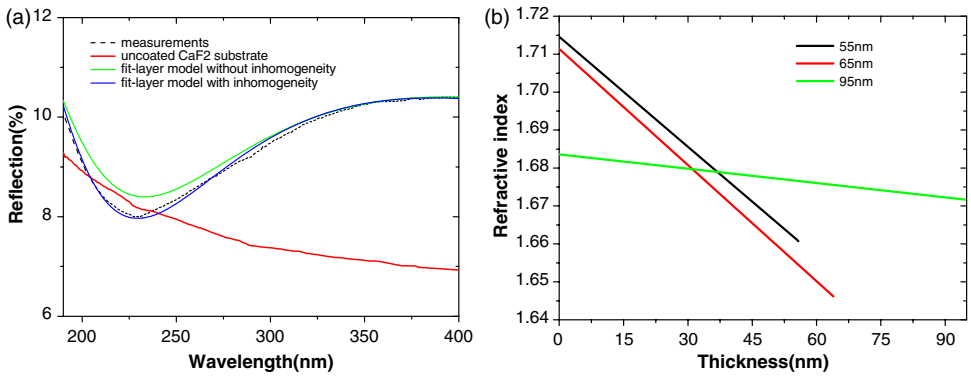

Fig. 1. (a) Reflectance fitting curves of LaF_3 thin films on CaF_2 and (b) refractive index variation with the thickness of LaF_3 single layer at 193 nm.

from Fig. 1(a) the fitting comparison of the reflectance curves of LaF_3 single layer with and without inhomogeneity that, obviously, the LaF_3 material exhibited a negative inhomogeneity (the refractive index decreased as the film thickness increased). Figure 1(b) shows that the refractive index varies with the thicknesses of LaF_3 single layer; different thicknesses of LaF_3 single layer give different optical constant results. This is because the surface mobility of LaF_3 molecules is particularly sensitive to the temperature, deposition rate, substrate surface quality, and so on [11,12]. The LaF_3 film becomes inhomogeneous with increasing thickness, so the refractive index of LaF_3 was carefully chosen and modified according to the required coating thickness during the deposition process. The refractive index of MgF_2 can be obtained through the normal dispersion model. The refractive index (n) and extinction coefficients (k) of LaF_3 and MgF_2 films at using deposition parameters are shown in Table 1.

B. Design Optimization

The penetrating effect in layer materials for *P*-polarized laser light is much stronger than the *S*-polarized light, especially in the DUV range, which will lead to a severe absorption problem. Absorption analysis of a random *P*-polarized AR coating design for each layer (layers 1 to 7, from substrate to air, respectively) is displayed in Fig. 2. The main absorption is caused from LaF_3 and the layers closer to the air have higher absorption.

The reason for that can be explained in the electric field distribution diagrams as showed in Fig. 3(a). The evaluation of the standing wave electric fields at oblique incidence for *P*-polarized light inside the designed films is shown by the electric field intensity as a function of physical thickness [13]. It reveals the electric intensity going stronger toward the layer–air interface direction and the *P*-polarized laser light penetrates throughout almost all the layers without much attenuation. The vital problem is to reduce the absorption loss of the AR coatings.

In order to reduce the absorption loss of the AR coatings, the thickness of the high refractive (LaF_3) material should be designed to a minimum. The AR coating for *P*-polarized laser beam at large AOI (68°–74°) was designed as follows: sub/43.5 nm (L), 30.2 nm (H), 50.2 nm (L), 30.0 nm (H), 50.3 nm (L), 29.4 nm (H), 1.6 nm(L)/air, with overall layer thickness of the high refractive layers of less than 90 nm.

Figure 3(b) shows the comparison between "standard 1/4 design" and "modified design." After adjusting the thickness of "HL" materials, the light path of the *P*-polarized laser in the H material is shorter and the electric intensity is lower than in the standard 1/4 design. The energy burden was shifted to the low material (MgF_2), which helps in increasing the laser-induced damage threshold (LIDT). A MgF_2 layer with thickness about 1.6 nm was used as the last layer to make a smoother and denser surface, which was proven in round-robin experiments, was absolutely necessary to increase the LIDT and long-term stability.

Table 1 Optical Constants of LaF_3 and MgF_2

Material	n (at 193 nm)	k (at 193 nm)
CaF_2	1.502	0
LaF_3	1.702	0.00325
MgF_2	1.421	0.000496

C. Analysis of Designed Results

In practice, selection of a sufficient coating design has not only to take the theoretical performance into account but also requires additional knowledge of their sensitivity to deposition errors. The refractive indices and thickness tolerance of the designed results are analyzed in detail by the merit function (MF) method to evaluate the designed results and optimize the depositing process [14]. The preproduction estimation of errors provides a statistical evaluation of the effect that errors in the layer refractive indices and thicknesses in a design will have on the spectral response of a designated

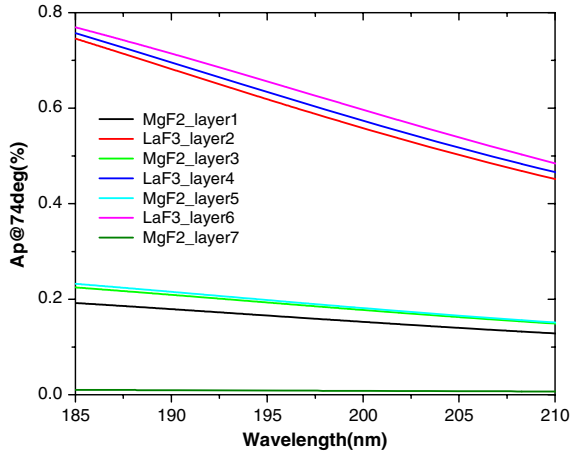

Fig. 2. Absorption of the *P*-polarized AR coatings for each layer (AOI = 74°)

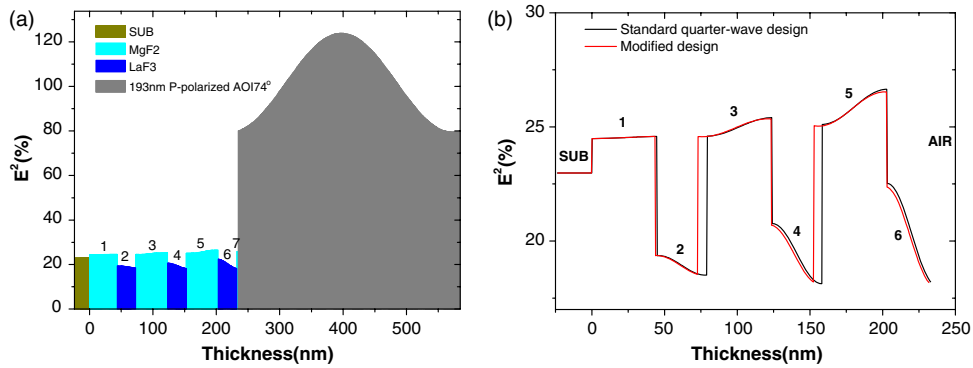

Fig. 3. (a) Electric field distribution in the *P*-polarized AR coatings and (b) electric field distribution comparison between "standard quarter-wave design" and "modified design" (zoom in) (AOI = 74°).

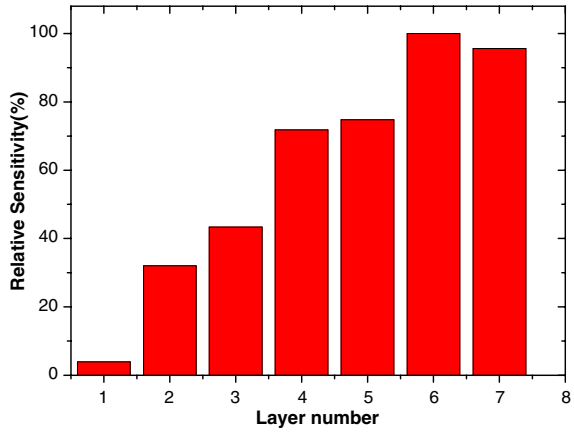

Fig. 4. Layer sensitivity with respect to thickness of the designed seven-layer AR coating.

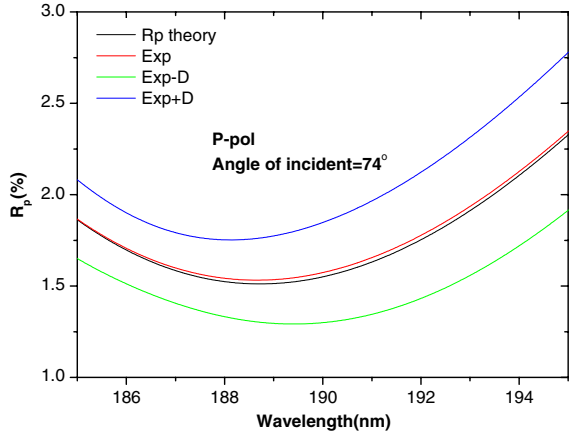

Fig. 5. Theoretical reflection R_p, mathematical expectation of reflection "Exp" and its corridor "Exp ± D" in the *P*-polarization case of the AR coatings at 74° AOI with the given 1% layer thicknesses and relative error levels of the refractive indices.

spectral characteristic. The relative sensitivity of thickness of the designed seven-layer AR coatings for each layer characterized by MF is shown in Fig. 4. As shown in Fig. 4 the sixth layer (layer 1 to 7, from substrate to air, respectively) is the most sensitive one, which means the most attention must be paid when depositing this layer.

Some statistical levels of error can be discussed as due to the corresponding processes. Certain values of the errors in refractive indices and thicknesses during the depositing process were assumed to get the corresponding changes of the spectral characteristic. The error sensibility of the designed coatings is shown in Fig. 5. Here "R_P theory" [the black (third) curve] refers to the original theoretical spectral characteristic of the designed seven-layer AR coating. The mathematical expectation is denoted as "Exp" in the red (second) curve and two curves [the blue (top) curve and the green (bottom) curve; these curves are denoted as "Exp ± D" in the graph, respectively] indicating the probability corridor for a given error level. The width of the probability corridor corresponds to the magnitude of the errors that were assumed as 68.3%. We can obtain from Fig. 5 that the mean value of reflection in the case of AOI equals 74° because *P*-polarized is 2.0% with the given 1% layer thicknesses and relative error levels of the refractive indices. The spectrum deviation of reflection is less than ±0.5%. This numerical estimation of possible variations is responsible for the comparison of sensitivities of different theoretical designs to manufacturing errors.

3. RESULTS AND DISCUSSION

A. Spectrum Test

The optical characteristics [angle resolved reflection (ARR), residual reflectance] of the AR coatings were assessed by a vacuum ultraviolet spectrometer (ML 6500 Metrolux) using *P*-polarized light [15]. The ARR method was applied to test the *P*-polarized AR coatings for AOI tolerance from 67° to 75°. It can be discerned from Fig. 6(a) that after coating the residual reflection is reduced dramatically in the range of 68°–74°. However, it is impossible to make the residual reflection very small throughout the whole working range of 68°–74° in the angular curve because of the large AOI. The R_P value increases sharply as the incident angle becomes bigger than the Brewster's angle. In the case of deviations of ±1° from the optimal AOI range (68°–74°), the residual reflection of AR coating for *P*-polarized at large AOI was lower than 3.9% in the angle range of 67°–75°. And the minimum residual reflection is at AOI of approximately 66°–71°; the residual reflection was less than 0.5% in that range.

As shown in Fig. 6(b) the results of residual reflection showed that the deviation between theoretical and measured ones was no more than 0.5%, which is in the error corridor of mathematical expectation. The residual reflection of *P*-polarized light at an incidence angle of 74° was below 2.5% in the range of 188–195 nm and achieved the minimum

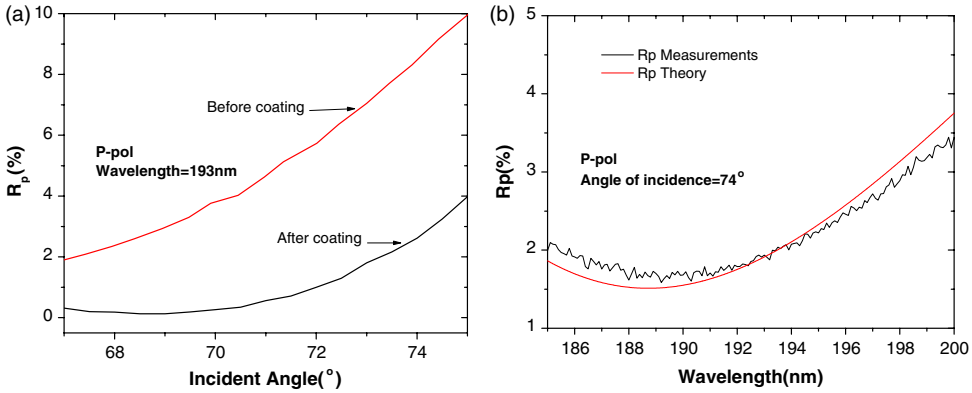

Fig. 6. (a) ARR and (b) residual reflection spectra of the AR coatings.

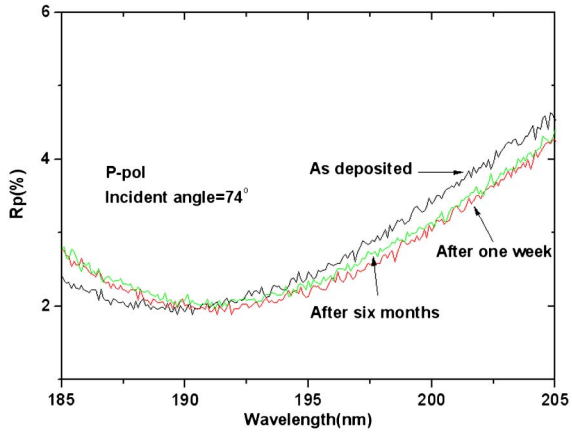

Fig. 7. Long term stability of *P*-polarized AR coatings for large AOI.

value of 2.0% at 193 nm, which is about 9.0% in original bare substrate. The residual reflection loss on the bare surfaces of optical components is reduced by 78%.

B. Stability and Endurance Test

Long-term stability and laser endurance resistance tests of the AR coatings were carried out to verify the durability of the coating against temperature and air humidity. The spectrum measurements were performed as deposited and repeated several times within half a year. Figure 7 shows that the spectrum of this AR coating converges to stable after one week. The resident reflection at the working wavelength of 193 nm hardly changes within six months (from 2.0% to 2.1%), and the slight wavelength shift to the longer wavelength is negligible.

Laser resistance tests were carried out using laser pulses with energy densities of approximately 25 mJ/cm^2. After millions of shots, the AR coatings show no layer degradation, tears, or other degradations, which verified the laser resistance of this coating.

4. CONCLUSIONS

The following factors are significant for successful fabrication: the proper use of inhomogeneous characteristics in the LaF_3 layer material; the compress of the LaF_3 thickness method in the design modified process; the last protective thin layer of MgF_2; and the preproduction estimation evaluation of the designed coatings. The AR coatings for *P*-polarized 193 nm laser light at large AOI (68°–74°) show promising results as known in open publications. The reflectance loss for *P*-polarized ArF lasers incident upon the bare optical surfaces in the range of 68°–74° is reduced dramatically. The impact of this improvement is a significant enhancement in output efficiency and lifetime of the optical components in the DUV range.

REFERENCES

1. D. Basting, G. Marowsky, and U. Brinkmann, *Excimer Laser Technology* (Springer, 2005).
2. R. Kuschnereit and H. Paul, "Antireflection coating for ultraviolet light at large angles of incidence," U.S. patent 6,697,194B2 (February 24, 2004).
3. R. M. A. Azzam, "Dividing a light beam into two beams of orthogonal polarizations by refection and refraction at a dielectric surface," Opt. Lett. **31**, 1525–1527 (2006).
4. K. Yang, X. Long, Y. Huang, and S. Wu, "Design and fabrication of ultra-high precision thin-film polarizing beam splitter," Opt. Commun. **284**, 4650–4653 (2011).
5. S. Wilbrandt, O. Stenzel, and N. Kaiser, "All-oxide broadband antireflection coatings by plasma ion assisted deposition: design, simulation, manufacturing and re-optimization," Opt. Express **18**, 19732–19742 (2010).
6. C. Görling, U. Leinhos, and K. Mann, "Comparative studies of absorptance behaviour of alkaline-earth fluorides at 193 nm and 157 nm," Appl. Phys. B **74**, 339–346 (2002).
7. E. Eva and K. Mann, "Calorimetric measurement of two-photon absorption and color-center formation in ultraviolet-window materials," Appl. Phys. A **62**, 143–149 (1996).
8. R. M. A. Azzam and N. M. Bashara, *Ellipsometry and Polarized Light* (North-Holland, 1987).
9. R. M. A. Azzam, "Tilted parallel dielectric slab as a multilevel attenuator for incident *P*- or *S*-polarized light," Appl. Opt. **48**, 425–428 (2009).
10. A. V. Tikhonravov, M. K. Trubetskov, and G. W. DeBell, "Optical coating design approaches based on the needle optimization technique," Appl. Opt. **46**, 704–710 (2007).
11. M. C. Liu, C. C. Lee, M. Kaneko, K. Nakahira, and Y. Takano, "Microstructure-related properties of lanthanum fluoride films deposited by molybdenum boat evaporation at 193 nm," Thin Solid Films **492**, 45–51 (2005).
12. M. Bischoff, D. Gäbler, N. Kaiser, A. Chuvilin, U. Kaiser, and A. Tünnermann, "Optical and structural properties of LaF_3 thin films," Appl. Opt. **47**, C157–C161 (2008).
13. J. H. Apfel, "Electric fields in multilayers at oblique incidence," Appl. Opt. **15**, 2339–2343 (1976).
14. S. A. Furman and A. V. Tikhonravov, *Basics of Optics of Multilayer Systems* (Editions Frontieres, 1992), p. 64.
15. P. Kadkhoda, H. Blaschke, J. Kohlhaas, and D. Ristau, "DUV/VUV spectrophotometry for high-precision spectral characterization," Proc. SPIE **4099**, 311–318 (2000).